



## Biosynthesis of Gold Nanoparticles using *Scytosiphon lomentaria* (Brown algae) and *Spyridia filamentosa* (Red algae) from Kyrenia Region and Evaluation of their Antimicrobial and Antioxidant Activity

### Girne Bölgesi'nden *Scytosiphon lomentaria* (Kahverengi algler) ve *Spyridia filamentosa* (Kırmızı algler) kullanarak Altın Nanoparçacıklarının Biyosentezi ve Antimikrobiyal ve Antioksidan Aktivitelerinin Değerlendirilmesi

Doga Kavaz<sup>1,2,3</sup>, Tariro Zimuto<sup>3</sup> and Huzaifa Umar<sup>1,2,3</sup>

<sup>1</sup>Department of Bioengineering, Institute of Graduate Studies and Research, Cyprus International University, Mersin, Turkey.

<sup>2</sup>Biotechnology Research Center, Cyprus International University, Mersin, Turkey.

<sup>3</sup>Bioengineering Department, Cyprus International University, Mersin, Turkey.

#### ABSTRACT

This study was carried out for biosynthesis of gold nanoparticles by using *Scytosiphon lomentaria* (brown algae) and *Spyridia filamentosa* (red algae) and compared. Synthesized gold nanoparticles were characterized using the UV-Vis spectroscopy (UV-Vis), Fourier transform infrared (FTIR) and Master Sizer analysis. Macro algae extract involvement in the stabilization of the gold nanoparticles was confirmed by the presence of UV-Vis peak at 540 nm and is an indication of the presence of the gold nanoparticles (AuNPs). Stretch in peaks of the FTIR showed that the biomolecules present in the seaweed extract reduced the gold ions. Master sizer results for AuNPs were within the range of 15-55 nm. Antioxidant activity carried out using 2,2-diphenyl-1-picrylhydrazyl (DPPH) free radical scavenging activity revealed significant activity for both AuNPs. Biosynthesized AuNPs also showed antimicrobial activity against *S. typhi* and *E. coli*. The *S. lomentaria* AuNPs exhibited inhibition against *E. coli*, whereas *S. filamentosa* gold nanoparticles showed antibacterial activity against *S. typhi*. Synthesized AuNPs using *S. lomentaria* and *S. filamentosa* extracts as stabilizing agents showed convincing antioxidant and antimicrobial activity against gram negative and gram positive bacteria.

#### Key Words

Nanoparticle preparation, Characterization, *S. filamentosa*, *S. lomentaria*.

#### ÖZ

Bu çalışma, *Scytosiphon lomentaria* (kahverengi yosun) ve *Spyridia filamentosa* (kırmızı yosun) kullanılarak altın nanopartiküllerinin (AuNPs) sentezi için yürütülmüş ve bu iki türden kullanılarak sentezlenen nanopartiküllerin karşılaştırması yapılmıştır. Altın nanoparçacıklar daha sonra UV-Vis spektrofotometre, FTIR ve Mastersizer kullanılarak karakterize edilmiştir. UV-Vis kullanılarak altın nanopartiküllerin oluşumu 540 nm'de oluşan pik ile görülmektedir. FTIR'daki gerilme, deniz yosunu ekstraktında bulunan biyomoleküllerin altın iyonlarını azalttığını göstermiştir. Mastersizer sonuçları, nanoparçacıkların 15-55 nm aralığında geniş bir dağılım göstermektedir. 2,2-diphenyl-1-picrylhydrazyl (DPPH) serbest radikal yöntemi kullanılarak gerçekleştirilen antioksidan aktivitesi, her iki nanopartikül için de önemli aktiviteler göstermiştir. *S. typhi* ve *E. coli* kullanılarak antimikrobiyal etkileri araştırılmıştır. *S. lomentaria* altın nanoparçacıklar *E. coli*'ye karşı inhibisyon sergilerken, *S. filamentosa* altın nanopartikülleri *S. typhi*'ye karşı inhibisyon göstermiştir. Stabilize edici ajan olarak kullanılan *S. lomentaria* ve *S. filamentosa* özütleri ile sentezlenen altın nanoparçacıklar, hem gram negatif hem de gram pozitif bakterilere karşı ikna edici antioksidan ve antimikrobiyal aktivite göstermiştir.

#### Anahtar Kelimeler

Nanoparçacık hazırlanması, karakterizasyonu, *S. filamentosa*, *S. lomentaria*.

**Article History:** Received: Jan 28, 2019; Revised: May 12, 2019; Accepted: Jul 11, 2019; Available Online: Nov 1, 2019.

**DOI:** <https://doi.org/10.15671/hjbc.518593>

**Correspondence to:** D. Kavaz, Bioengineering Department, Cyprus International University, Mersin 10, Turkey.

**E-Mail:** dkavaz@ciu.edu.tr

## INTRODUCTION

Nanotechnology is rapidly expanding with it serving the main purpose of manufacturing materials at nanoscale although having the same application as the normal size material. Nanotechnology is defined as a study of techniques of materials manipulation in the range from 1-100nm such as from the size of a single atom up to those of traditional chemistry [1]. It has become an important part of the livelihood of most living organisms. Nanotechnology has led to a huge revolutionary change in science, having great technological achievements and employment of people with great expertise and experience, thus encompassing both practical and theoretical science. The nanoparticles are chosen and synthesized based on their different properties which make them suitable for the purposes they serve [2]. The synthesis of nanoparticles can be achieved by some physical and chemical methods. The traditional and commonly used method for nanoparticles synthesis is wet method. Nanoparticles have become the hope for the future as they are now synthesized and utilized in different ways [3]. The utilization of nanoparticles is increasing due to their increased surface area to volume ratio. Studies have been carried out in different fields to observe the various properties and characteristics of the nanoparticles. During these past few decades, further studies of these nanoparticles has shown their integrated biological properties such as antitumor, antimicrobial and anti-HIV activities [4].

Simultaneously, nanotechnology has evolved as a subdivision of green innovation or eco-innovation technologies, which allows for application in various aspects that support “green growth” and excellent perspectives for social and economic development [5]. With the introduction of biosynthesis of nanoparticles, the high demand of the nanoparticles can now be overcome without any damage being done to the environment. The aim for green innovation is to produce new nanoparticles using various biological entities and eco-friendly recyclable materials. This brings about new production procedures and purchase modalities thus, reduction in work space, work load (because of the one pot synthesis), labor is reduced, and the use of hazardous chemicals [6]. The significantly new methods of synthesis are also aimed at addressing the health and environmental safety of the formation and utilization of the nanoparticles.

Biological entities are being considered and tried for the green synthesis of many nanoparticles with their different applications. Among the different biological entities being investigated for biosynthesis is macro algae which are also called bionanofactories because they synthesize nanoparticles with high stability and eliminate cell maintenance. Algae are naturally available and are a very important source of phytochemicals involved in the synthesis of metallic nanoparticles. Seaweeds have shown a wide spectrum use in the medical field [7]. They are a good source of bioactive compounds which have a wide range of biological applications that include anticoagulant, antifouling and antibacterial activity [8]. Seaweeds have been used since ancient times for medicinal purposes as an anthelmintic and aesthetics. They were used as antibiotics in the treatment of gout, wounds, cough, hypertension and even some venereal diseases. Recent literature has also shown that macro algae can be used in the treatment of hypertension, cancer, allergy, oxidative stress, thrombosis, lipidemia and some degenerative diseases [9].

Green synthesis is being adopted by scientists because it has proven to have lesser after effects to human and animals when using the products [10]. It is also reliable because it is simple, easy, environmentally friendly and less laborious. Synthesis gold nanoparticles using this method has a greater advantage and it is a fast one-step biosynthesis method [11]. The biosynthesized nanoparticles also exhibit a unique particle size. Thus, the green synthesis of nanoparticles is dependent on shape, physical, chemical and biological properties [12]. The gold nanoparticles are used for the development of biosensors, DNA labeling and vapor sensing [13-15] and gold nanoparticles also applied to the determination of ct-DNA and used as potential biological labels [16].

In this study, stable and eco-friendly green synthesis of gold nanoparticles using *S. lomentaria* and *S. filamentosa* aqueous extract as a stabilizing agent and their characterization done using various spectroscopic techniques was also reported. Antioxidant activity of the synthesized nanoparticles was carried out DPPH free radical scavenging activity and antimicrobial activity against *E. coli* and *S. typhi* using disc diffusion method.

## MATERIALS and METHODS

### Chemical Reagents

Potassium tetrachloroaurate ( $\text{KAuCl}_4$ ), Nutrient agar, Nutrient broth, Antibiotics, distilled water, ethanol, barium chloride and sulphuric acid. All chemicals used in the experiment were ACS-reagent grade, produced by Sigma (St. Louis, MO, USA).

### Sample Collection

The algal species were collected from the Kyrenia harbour which is along the coastline of the Mediterranean Sea. The samples were collected and stored in polythene bags and taken to the laboratory for classification. The species that were collected were *S. lomentaria* and *S. filamentosa*. The samples were then stored in a cool place until they were used for preparation of the algal extracts.

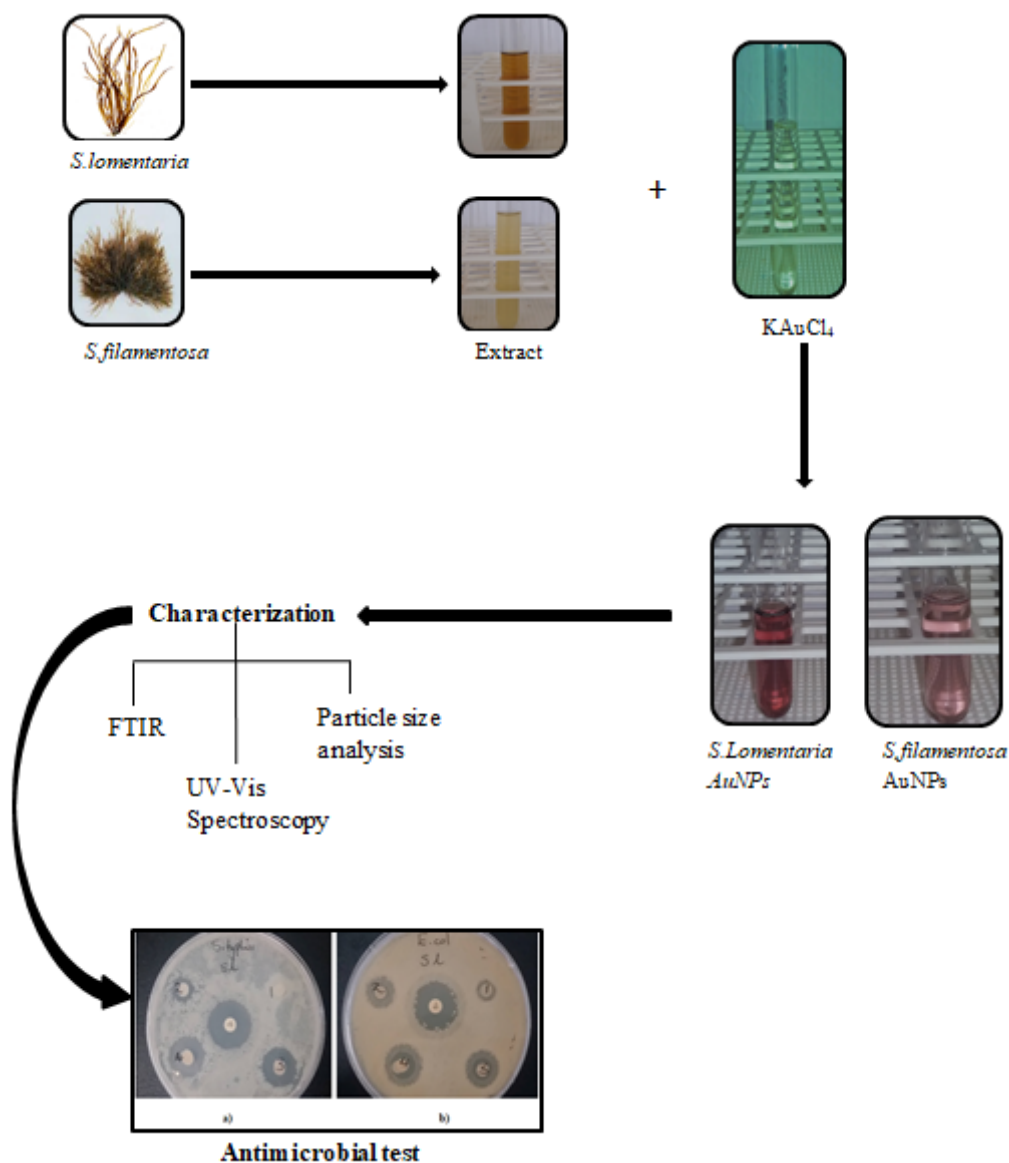


**Figure 1.** The overview of synthesis, characterization and antibacterial activity of gold nanoparticles using *S. lomentaria* and *S. filamentosa* extract.

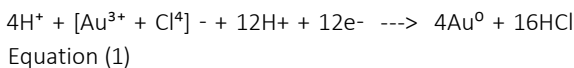
The flow chart shows a summary of the process from the collection of the seaweed and the preparation of the extract solutions. The extract solution are then mixed with the potassium tetrachloroaurate at a certain ratio to produce the nanoparticles and characterization was then done using the FTIR, UV-Vis spectrophotometer and the Mastersizer. The antibacterial test was then done using the disc diffusion method.

### Preparation of Extract

The seaweeds were washed with tap water to remove other marine organisms and epiphytes. They were rinsed with distilled water and then placed in the oven to dry at 45°C. The samples are ground into a powder using a pestle and mortar. The algae powder was mixed with ethanol at a ratio of 1:15 (w/v) and poured into the soxhlet apparatus. The extraction process was done at 50°C for 8 hours. After extraction the solvent was then evaporated at a temperature of 40°C using rotary evaporator. The *S. lomentaria* extract was brown in color and the *S. filamentosa* extract is yellowish as shown in Figure 1 is then kept at 4°C in refrigerator for further use.

### Synthesis of Gold Nanoparticles

Potassium tetrachloroaurate (KAuCl<sub>4</sub>) purchased from Sigma-Aldrich was the source of the Au<sup>3+</sup>. The potassium tetrachloroaurate is dissolved in distilled water to make a solution that is 2.5×10<sup>-4</sup>M in concentration. For synthesis as shown in Figure 1, 22.5 ml of potassium tetrachloroaurate is added into a beaker and it is heated to 100°C and stirred vigorously. 7.5 ml of seaweed extract was measured using a graduated syringe and added to the KAuCl<sub>4</sub>. The solution is continuously stirred for about 10 minutes and the color change is observed. The synthesis is repeated at different time intervals and temperatures. The UV-Vis spectroscopy is carried out at the different intervals to monitor the progress of the reaction. For time intervals the UV-vis spectrum was recorded at 5 min, 10 min, 15 min, 20 min, 25 and 30 min whereas for temperature intervals, the synthesis is carried out at 25°C, 50°C, 75°C and 100°C. This was done for both seaweed samples. The chemical equation for this reaction is:



### Characterization of Synthesized Gold Nanoparticles

The synthesis of the AuNPs and kinetic behavior was monitored by the UV-Vis spectrophotometer by analyzing formation of the surface resonance peaks. The scanning range of the nanoparticles is 400-800 nm at a scanning speed of 480 mm/min. The FT-IR was done to analyze the presence of the phytochemicals in the extracts used in the biosynthesis. Small aliquots of the concentrated reaction mixture are measured after the reaction in the mode at 400-4000cm<sup>-1</sup>. The spectra were recorded and the analysis was also carried out

after the synthesis of the AuNPs and the spectra are then analyzed. Nanoparticle size was measured using the Malvern Mastersizer 2000 particle size analyzer. Crystalline structure was analyzed using X-ray diffractometer (Rigaku ZSX Primus II).

### Antioxidant Activity of the Synthesized Gold Nanoparticles

The effect of extracts on DPPH radical was estimated by DPPH radical scavenging assay using the method of Znati et al. [17] with slight modification. Solution of 0.135 mM DPPH in methanol was prepared and 1.0 ml of this solution was mixed with 1.0 ml (1:1 ratio) of nanoparticles suspension in methanol containing (20, 40, 60, 80, 100 g/ml) of the nanoparticles. After 30 min at 25°C incubated in darkness, the absorbance of each sample is measured at 517 nm. Blank is prepared by mixing 0.5 ml of DPPH solution with 0.5 ml of ethanol. A positive control of Gallic acid is prepared to compare the results of decreased absorption induced by the samples. The following equation is used to calculate the capability to scavenge 50% of DPPH, which is the percentage of inhibition (Equation 2).

DPPH scavenging effect / Inhibition ratio (%) =

$$\left[ \frac{(A_{\text{control}} - A_{\text{sample}})}{A_{\text{control}}} \right] \times 100$$

(Equation 2)

All tests are carried out in triplicate. A control stands for the absorbance for all the reagents except the tested sample. A sample stands for the absorbance of the test sample.

### Antimicrobial Activity

#### Minimum Inhibitory Concentration

This technique is done to deduce the minimum amount of AuNPs that can inhibit the growth of bacteria. Different concentrations of gold nanoparticles were prepared (25 µl, 50 µl, 75 µl and 100 µl). The bacteria (*S. typhi* and *E. coli*) were then cultured in the nutrient broth and the AuNPs was also added. Nutrient broth with bacteria only and another without the bacteria served as the controls. The bacterial cultures were then incubated at 37°C for 24 hours and then the results were recorded.

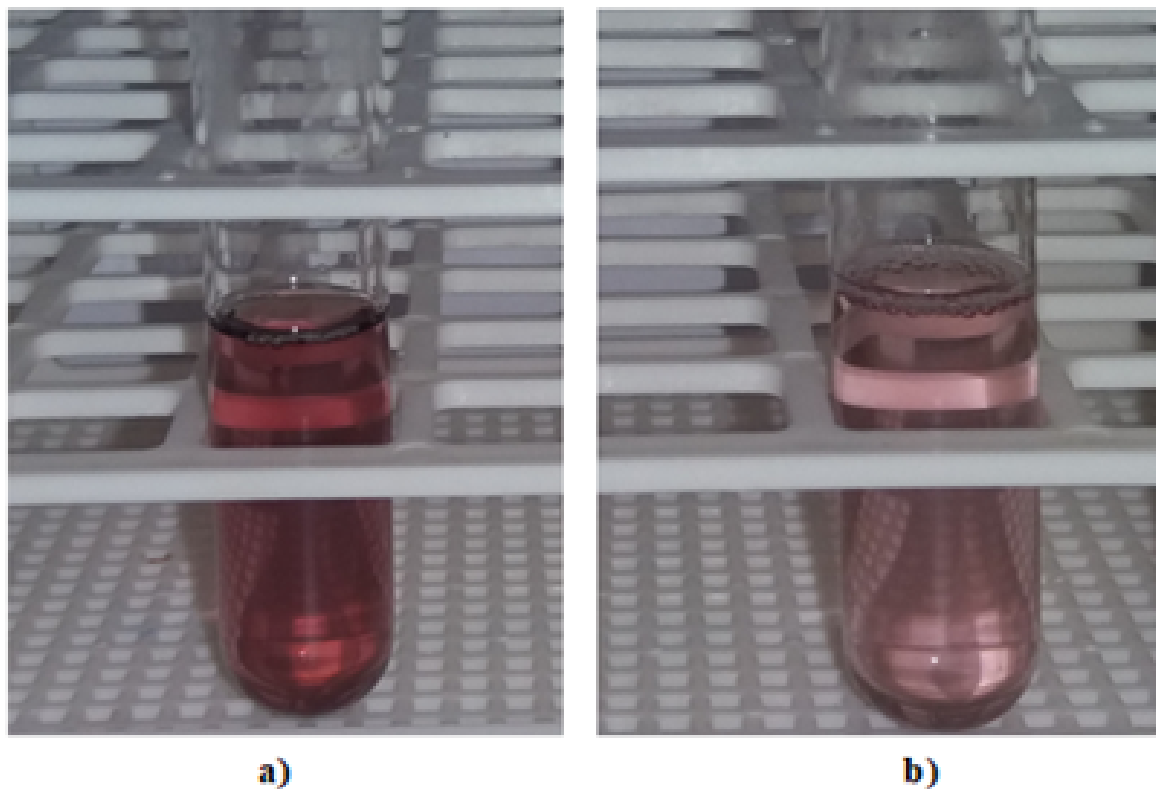


**Figure 2.** The color of the gold AuNPs synthesized using a) *S. lomentaria* and b) *S. filamentosa*. The solution of the gold nanoparticles synthesized using *S. lomentaria* species showed a ruby red color and that of gold nanoparticles synthesized using *S. filamentosa* species exhibited a pink color.

### Zone of Inhibition

Antibacterial activity analysis was carried out using disc diffusion method, in which a loop was used to take the bacterial solution and swab it on the surface of the media. The discs impregnated with the gold nanoparticles (100 $\mu$ l per disc in 6mm in diameter) and allowed to dry before they were placed onto the surface of the petri dishes using forceps. The dishes with bacteria were then incubated at 37°C for 24hours. The antibiotics ciprofloxacin were used as the positive control. After 24hours the clear zones around the discs were measured and expressed in millimeters and this is known as the zone of inhibition.

### Statistical Analysis

Data were analyzed with one-way analysis of variance (ANOVA). The significant difference among the mean values was examined by Duncan's test ( $P \leq 0.05$ ) with SPSS 13.0 software (SPSS Inc., Chicago, USA).

## RESULTS and DISCUSSIONS

### Biosynthesis of AuNPs and UV-vis spectroscopy

The formation and presence of bio reduction was confirmed by the color changes that take place within a few minutes after addition of the seaweed extract. Initially on a ratio of 1:1 the color of the solution was purple and the gold nanoparticles formed were relatively large after few adjustments were made to the experimental parameters and the reactants. The color of the solution changed to pink and ruby red following the mixing of extract and the gold at a ratio of 1:4 as shown in Figure 2 for both species *S. filamentosa* (SF) and *S. lomentaria* (SL) respectively, which is a characteristics of AuNPs [18]. Change in the color of the solution to pink and ruby confirmed the synthesis of AuNPs with respect to reaction time and temperature nanoparticles was seen in Figure 2. Increased in the color intensity as well as absorbance increase has to do with reaction time and temperature [19]. AuNPs formation was confirmed by the rapid appearance of red or pink color, which has to do with bio reduction of Au (III) ions due to excitation

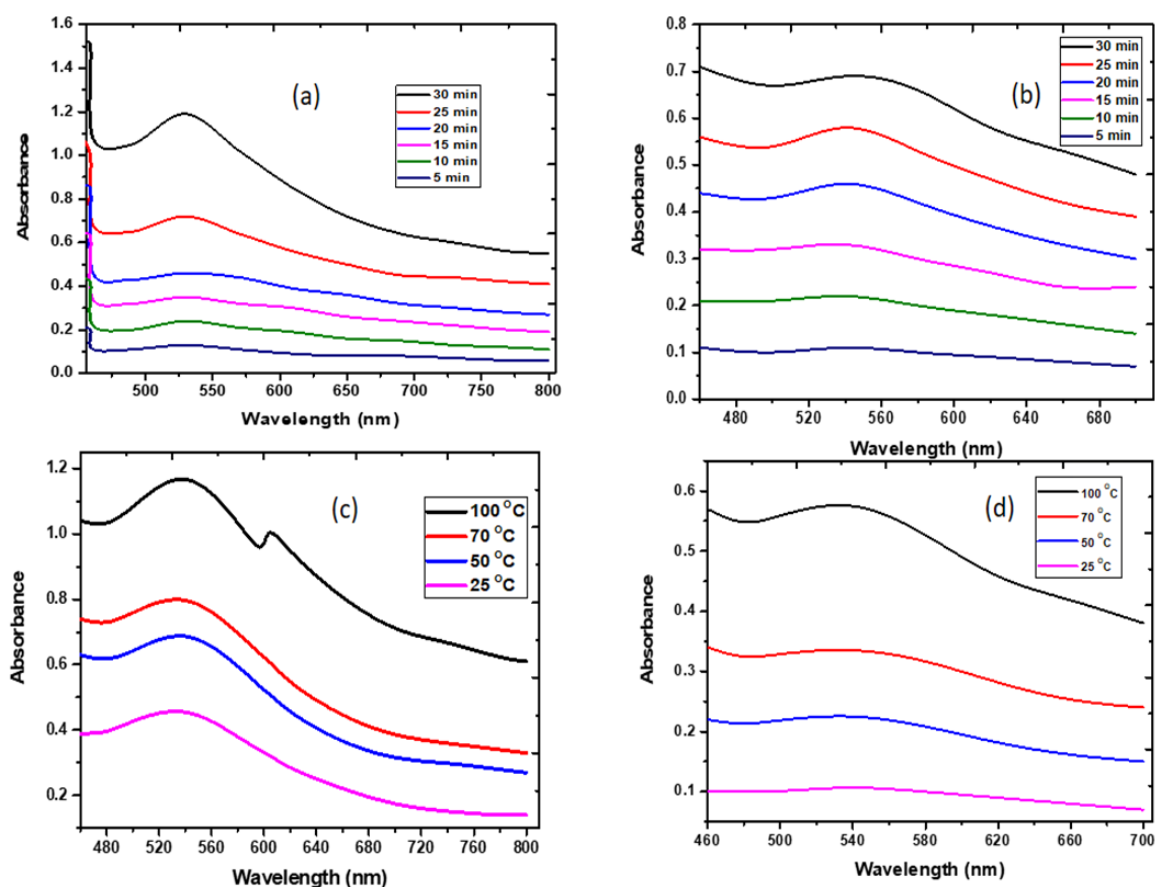


**Figure 3.** (a) UV-Vis spectrum of gold nanoparticles synthesised using *S. lomentaria* with respect to time. (b) UV-visible spectrum of gold nanoparticles synthesized using *S. filamentosa* with respect to time (c) UV-Vis spectrum of gold nanoparticles synthesized using *S. lomentaria* with respect to time (d) UV-visible spectrum of gold nanoparticles synthesized using *S. filamentosa* with respect to temperature.

of surface plasmon resonance in the gold nanoparticles [19].

The synthesis of AuNPs using *S. lomentaria* and *S. filamentosa* extract was demonstrated by the subsequent color changes that took place in the reaction mixture. The color of the gold nanoparticles synthesized using *S. lomentaria* change from yellow to ruby red and that of the synthesis using *S. filamentosa* changed to pink [20]. The color of the AuNPs change directly from yellow to red or sometimes pink is as a result of surface plasmon resonance excitation in the AuNPs which was observed and confirmed using the UV-Vis spectral evaluation [21].

Shift in SPR of the AuNPs in relation with time interval and temperature change (Figure 3a-d). Absorbance and color intensity values gradually changes with the reaction time which has to do with AuNPs increased as observed, and it also leads to continuous reduction of Au ions

as observed. Characteristic SPR absorption peaks at 532 nm confirms the formation of nanoparticles.

The reaction mixture with an excitation of the surface plasmon resonance recorded of 540 nm at the higher temperatures as shown in Figure 3a-d. The reaction time is prolonged with respect to decrease in temperature, at lower temperature, the reaction time is prolonged and the absorption spectra show a gradual increase of the absorbance shift in the  $\lambda_{max}$  from 550 nm to 540 nm. Additionally, effect of temperature on the stability of *S. lomentaria* AuNPs was investigated by heating the nanoparticles at 80°C for 30 min. Furthermore, increase in temperature would lead to the production of AuNPs that are stable under a wide range of environmental factors and this enabled them to study their potential effectiveness and safe therapy. Thus, the stability of the *S. lomentaria* AuNPs made it easier for the storage of the nanoparticles for use during the antimicrobial test

[22]. Increase in temperature resulted in the shifting of the  $\lambda_{max}$  to longer wavelengths. Thus, at temperature above 50°C leads to further increase in the absorption indicating the formation of smaller nanoparticles. The absorption maximum is attributed by the surface plasmon resonance. There is a smaller change in absorbance when the temperature is increased from 50°C to 70°C which indicates there is a slight change in size of the gold nanoparticles. On the other hand big gaps are visible when the temperature is increased from 25°C to 50°C and from 70°C to 100°C indicating an increased in the reaction speed.

Temperature affects the size of the nanoparticles and the rate of the reaction. The gold nanoparticles produced for both extract at higher temperature are highly stable and can be stored for some days without any change. The maximum absorption of gold nanoparticles with respect to temperature ranges from 536 to 545 nm. Furthermore, there was a slight increase in the absorbance maxima which indicates the production of large nanoparticles at lower temperatures. Thus, at a higher temperature, the reduction was faster and it was observed by the change in color and the mixture with an excitation of the surface plasmon resonance at 536 nm. This can be compared to the synthesis of gold nanoparticles using *P. tetrastromatica* which showed that

smaller nanoparticles where synthesized at high temperature of 80°C and the UV-Vis spectra peaks where in the range of 55-540 nm [23, 24].

Surface plasmon bands of the gold nanoparticles are broad with an absorption tail in the longer wavelength region that extends well into the near infrared region of the colloids synthesized at different temperatures. The absorption maxima for the gold nanoparticles were obtained for the least values (535-543 nm) without any other absorption band in the longitudinal plasmon resonance (Figure 3d). Additionally, significant increase in the intensity of the absorption peak is noted. Initially, at 5 minutes there is slight to no reaction at all and the color solution remains gold the absorption peak is at approximately 540nm. Color starts to change gradually with change in time, and there is a slight shift in the absorption peak at 10minutes. Furthermore, color change was also observed over time as the color change starts taking place after 10 to 15 minutes and the solution starts turning into a pale pink color. Increase revealed some significant peak shifts which is attributed by the surface plasmon resonance band of the gold nanoparticles.

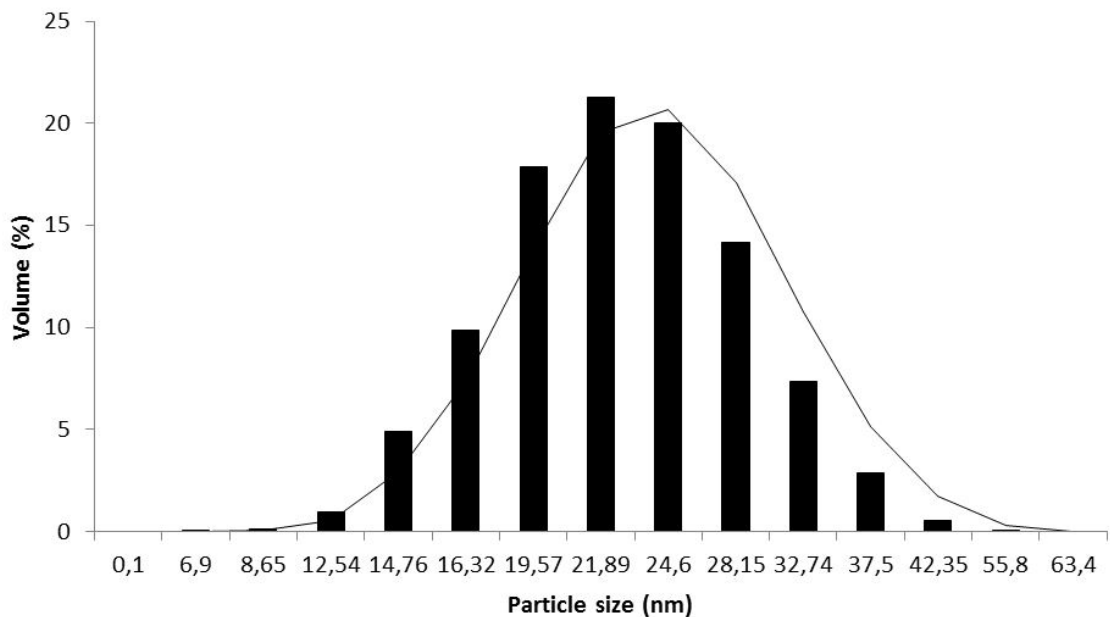


**Figure 4a.** Mean average particle size distribution of the *S. lomentaria* species. The graph is representation of data as mean values of the particle size and the experiment with n=3 replicates of the experiment. The graph also shows the trend line for the particle size distribution filamentosa with respect to temperature.

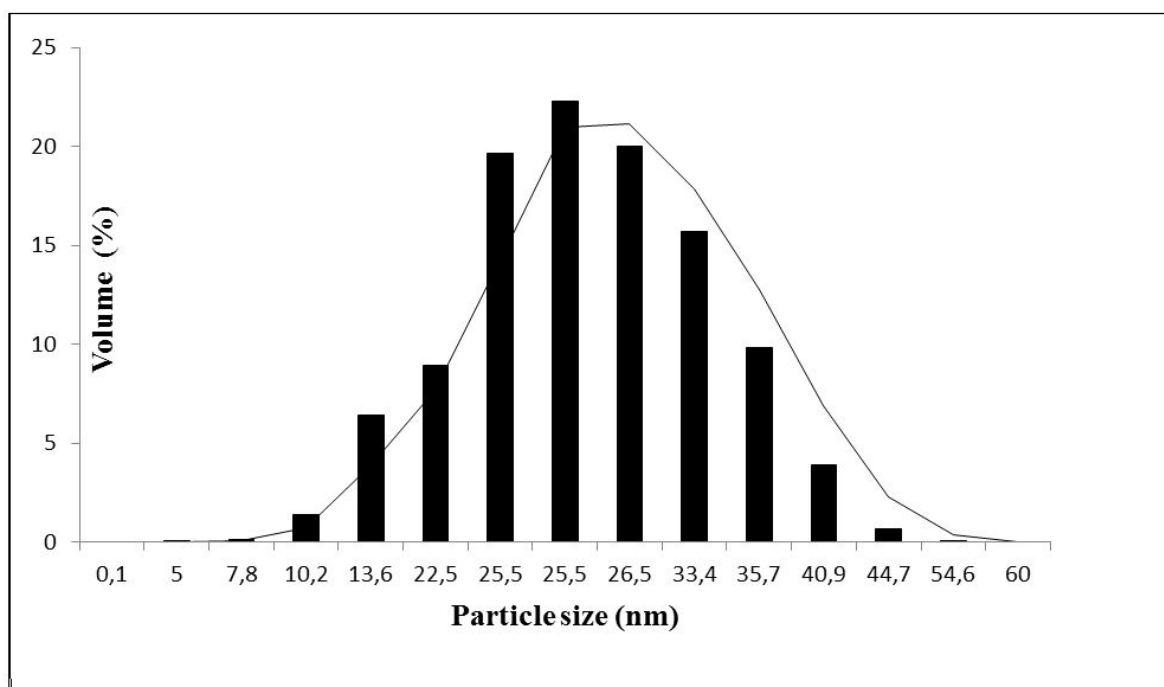


**Figure 4b.** The average particle size distribution of AuNPs synthesized using *S. filamentosa*. The graph represents data as mean values of the particle size and the experiment with  $n=3$  replicates of the experiment. The graph also shows the trend line for the particle size distribution.

#### Fourier transform infrared (FTIR) Studies

FTIR analysis of AuNPs were carried out at 25°C to identify the type of the biological molecules present in the AuNPs synthesized using *S. Lomentaria* and *S. filamentosa* extracts as reducing agents. The FTIR was analyzed at a range of 500 and 4000  $\text{cm}^{-1}$ . Synthesized AuNPs using *S. Lomentaria* and *S. filamentosa* revealed FTIR spectra, which show the composition of the molecules of *S. Lomentaria* and *S. filamentosa* and their distribution on the AuNPs surface.

Stretch of the peak at 3275  $\text{cm}^{-1}$  is a characteristic of the O-H bond in *S. Lomentaria* (Figure 5a), which stretches to 3292 after the bio reduction of the gold solution to form gold nanoparticles using *S. Lomentaria* (Figure 5c). This peak has a broad trough and this peak is present in both spectra because the O-H bond is still present even after the bio reduction of the gold solution [18]. The appearance of the peak at 1622  $\text{cm}^{-1}$  is characteristic of the C=O bond (carbonyl). The peak at 3275  $\text{cm}^{-1}$  represent the presence of organic compounds in the both the extract and the gold nanoparticle solution. This indicates the presence of amide bonds in the extract solution. Presence of the amide bonds after reduction is also shown by the stretch of peaks after reduction at 1630  $\text{cm}^{-1}$  and 1900  $\text{cm}^{-1}$ . Study has also shown the gold

nanoparticles were synthesized using *Turbinaria conoides*, the FTIR results showed the presence of amines, polyphenolic and carboxylic groups in the algae extract [18]. The groups are responsible for the reduction of the gold ions just like the *S. lomentaria* extract. The strong bands at 1042  $\text{cm}^{-1}$  and 1080  $\text{cm}^{-1}$  are caused by the vibrations of the C-OH bonds which are single bond absorption that can either be caused by the presence of proteins or certain glucosides. The peak at 2976  $\text{cm}^{-1}$  corresponds with presence of C-H bonds. The weak aromatic C-H bonds are also represented by the 876  $\text{cm}^{-1}$  and 590  $\text{cm}^{-1}$ . Additionally presence of carboxyl groups as identified by FTIR were involved in the gold recovery with the brown alga (*Sargassum polycystum*) and proposed the formation of oxygen bridges between gold and these groups [25].

The FTIR spectrum result shows bands represented by the bond vibrations and stretch caused by the biomolecules present in both *S. lomentaria* and *S. filamentosa*. After bio reduction of the gold solution, FTIR spectrum shows stretch of the functional groups represented by the bands formed as a result of stretch and vibrations after the formation of new bonds. Some of the functional groups represented by the bands are carboxylic acids, hydroxyl, carbonyls and amines.

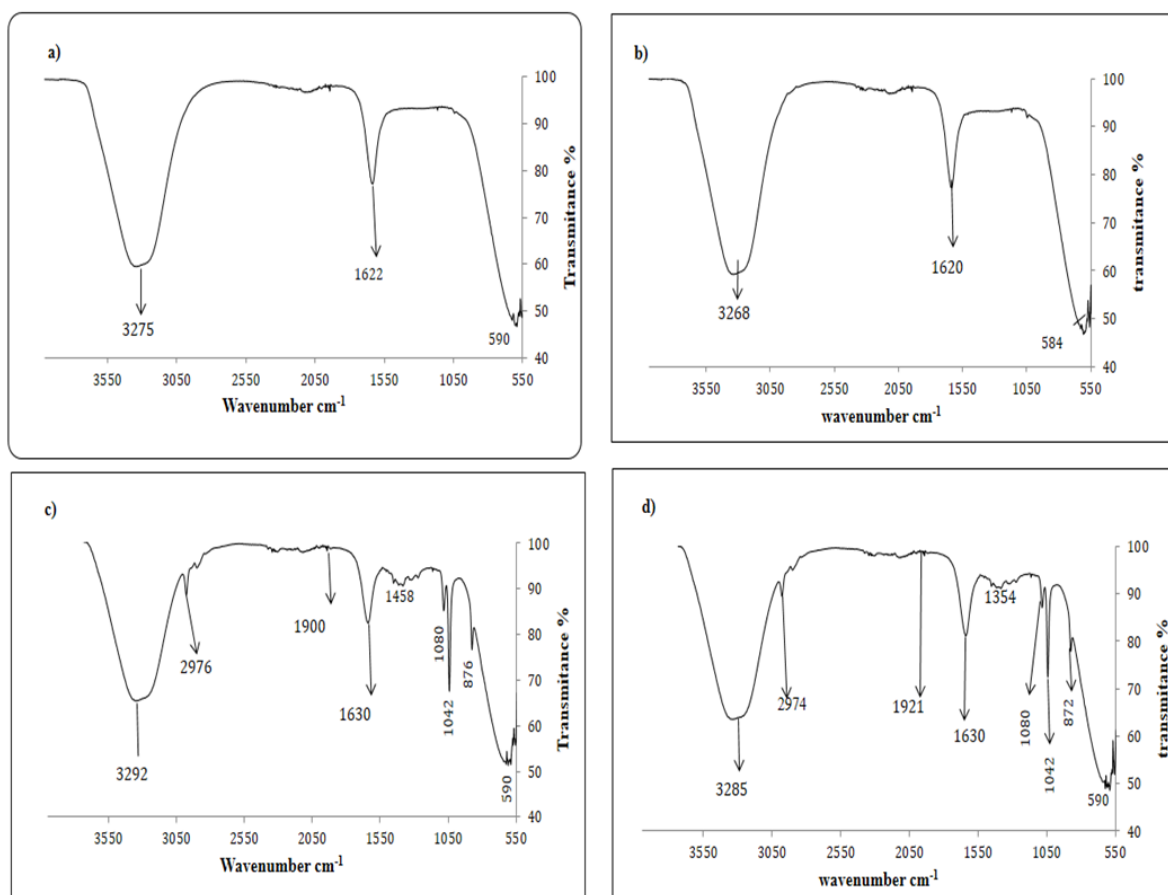


**Figure 5.** FT-IR spectra showing the bands of (a) *S. lomentaria* extract (b) *S. filamentosa* extract (c) Gold nanoparticles synthesized using *S. lomentaria*. (d) Gold nanoparticles synthesized using *S. filamentosa*. The FTIR spectrum result shows bands represented by the bond vibrations and stretch caused by the biomolecules present in both *S. lomentaria* and *S. filamentosa*. After bio reduction of the gold solution, FTIR spectrum shows stretch of the functional groups represented by the bands formed as a result of stretch and vibrations after the formation of new bonds. Some of the functional groups represented by the bands are carboxylic acids, hydroxyl, carbonyls and amines.

The stretch of the peak at  $3268\text{ cm}^{-1}$  is a characteristic of the O-H bond in *S. filamentosa* (Figure 5b), which stretches to  $3285\text{ cm}^{-1}$  after the bio reduction of the gold solution to form gold nanoparticles using in *S. filamentosa* (Figure 5d). The stretch at  $1630\text{ cm}^{-1}$  and  $1921\text{ cm}^{-1}$  give rise to the possible presence of the carbonyl (C=O) group which means there are amide bonds present in both the extract and the gold nanoparticle solution. The peak at  $2974\text{ cm}^{-1}$  corresponds with the C-H bonds present in the gold nanoparticle solution. The peaks resemble the presence of flavonoids, phenolics, flavones and terpenoids. There are also the presence of the aromatic carbons that are shown by the bands at  $1042\text{ cm}^{-1}$  and  $1080.13\text{ cm}^{-1}$ . The bands at  $872$  and  $590\text{ cm}^{-1}$  represent weak aromatic C-H bonds. In a study on the synthesis of gold nanoparticles using *P. tetrastromatica*, the FTIR showed that the extract contained functional group that might relate to some sugar molecules [23].

### XRD Results

The result of XRD pattern analysis of AuNPs using Cu K $\alpha$  radiation ( $\lambda = 1.54184\text{ \AA}$ ) in  $2\theta$  at a range of  $100$  to  $1000$  (scan speed of  $30\text{ min}^{-1}$ ), which revealed the Bragg's reflections at  $2\theta$  values of  $39.579$ ,  $46.567$ ,  $64.610$ ,  $77.546$  and  $79.700$ . Similarly, the Bragg's reflections at  $2\theta$  values represented [200], [111], [311] and [220] planes respectively, that confirmed the crystalline nature of gold with cubic face centered (FCC) structure of AuNPs (Figure 6a). Presence of those peaks confirm the formation of highly purified AuNPs without any impurity. Additionally, the pattern shows that the AuNPs was obtained from natural sources.

The XRD pattern obtained for gold nanoparticles synthesized using *S. lomentaria* exhibits Bragg reflections, which could be well manifested on the basis of the face centered cubic (FCC) gold nanostructures. The

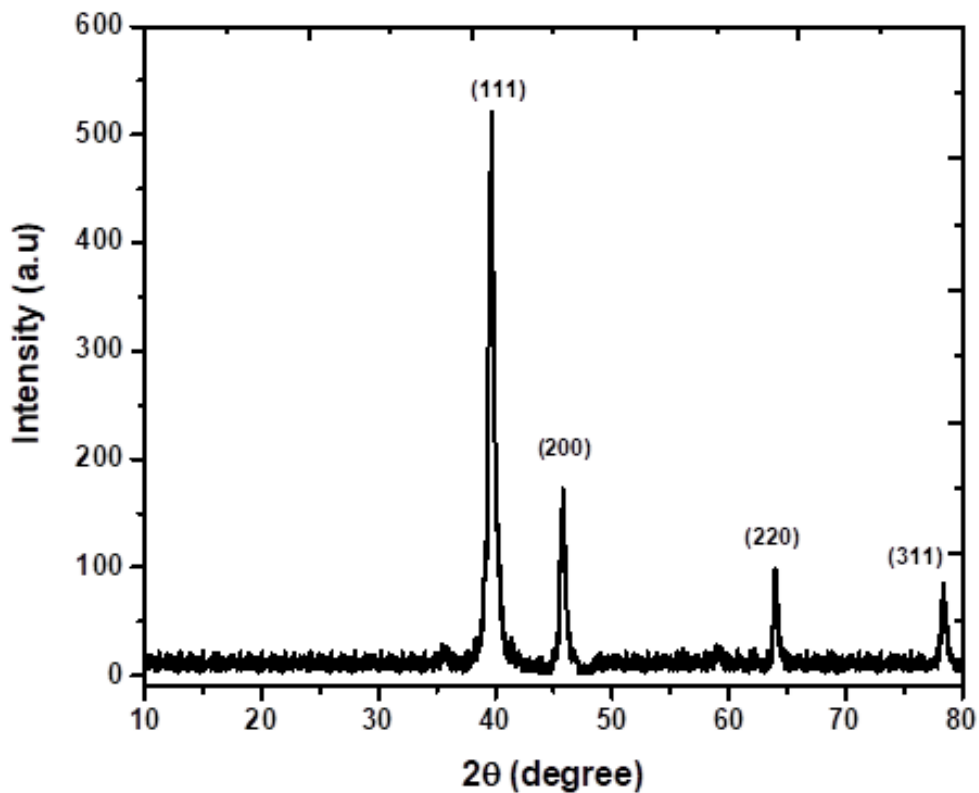


Figure 6a. XRD of gold nanoparticles synthesized using *S. filamentosa*.

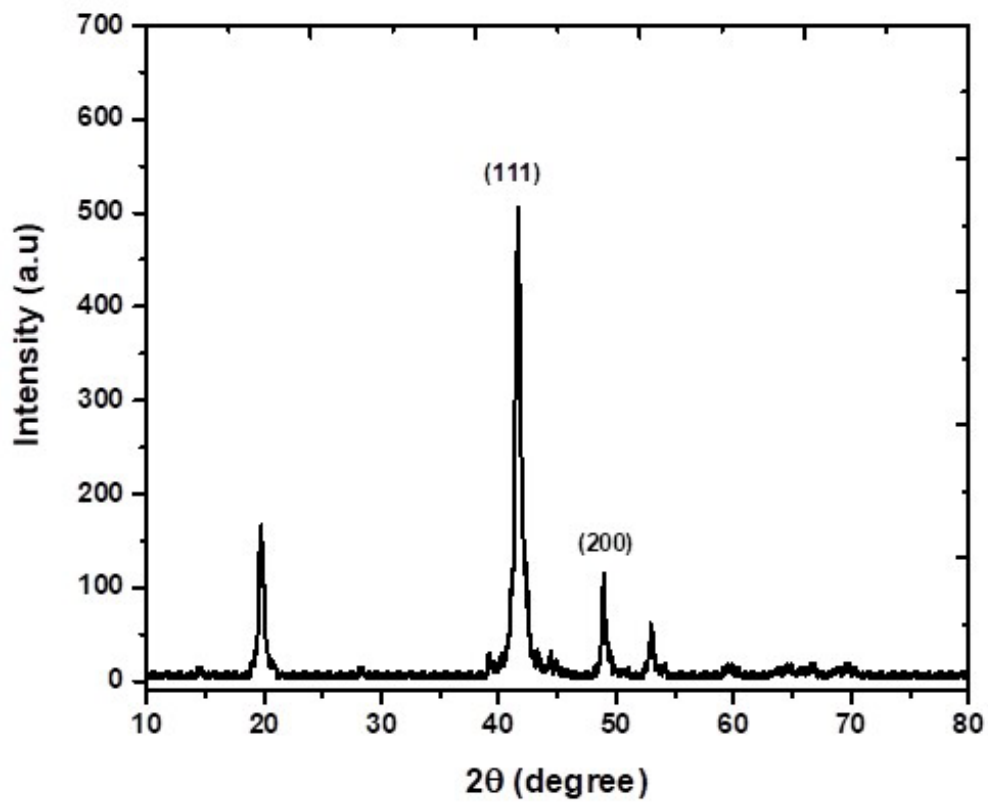


Figure 6b. XRD of gold nanoparticles synthesized using *S. lomentaria* aqueous extract.

**Table 1.** Minimum inhibitory concentration using different concentration.

	Sample	<i>E. coli</i>	<i>S. typhii</i>
Nutrient Broth	NB	-	-
	NBB	+	+
<i>S. filamentosa</i> AuNPs	25 µl	+	+
	50 µl	+	+
	75 µl	-	+
	100 µl	-	-
<i>S. lomentaria</i> AuNPs	25 µl	+	+
	50 µl	+	+
	75 µl	-	-
	100 µl	-	-

The Minimum inhibitory concentration was done with:- NB: - Nutrient broth only. NBB:-Nutrient broth cultured with bacteria. +:- Stands for bacterial growth. - : stands for no bacterial growth.

The volume of nanoparticles that is put on to the discs was 25 µl, 50 µl, 75 µl, and 100 µl. The minimum amount of gold nanoparticles required to inhibit the growth of bacteria was 75µl.

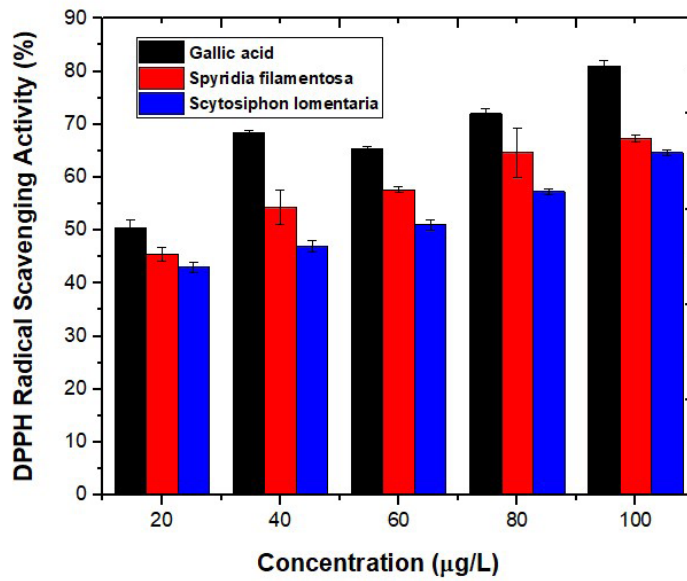


**Figure 7.** DPPH free radical scavenging activity of biosynthesized AuNPS using *S. filamentosa* and *S. lomentaria*.

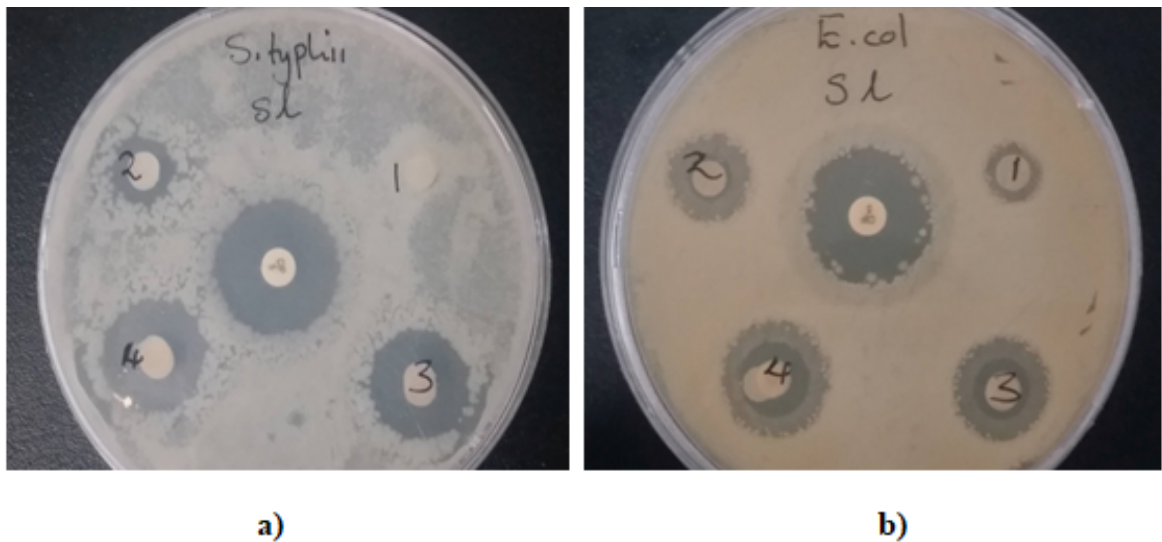


**Figure 8a.** Diagram showing disc diffusion method for *S. lomentaria* AuNPs against a) *S. typhii* and b) *E. coli*.

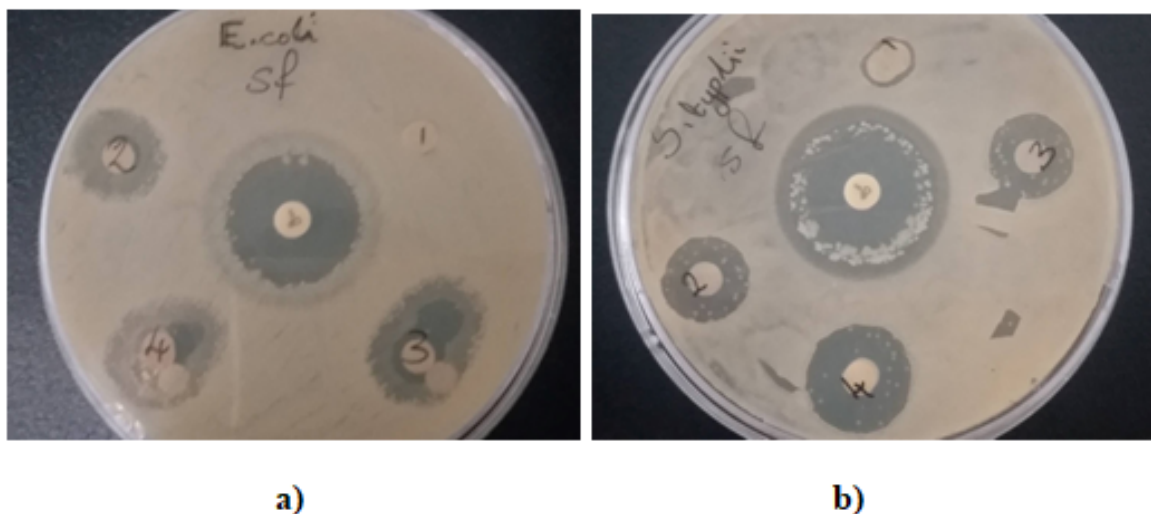


**Figure 8b.** Diagram showing disc diffusion method for *S. filamentosa* AuNPs against a) *E. coli* and b) *S. typhi*.

The antibacterial activity assay was carried out with the Antibiotics at the center, 1) negative control, 2) Extract, 3) KAuCl<sub>4</sub>, 4) AuNPs as shown by figure 20 and 21 respectively. The experiment was carried out in triplicate.

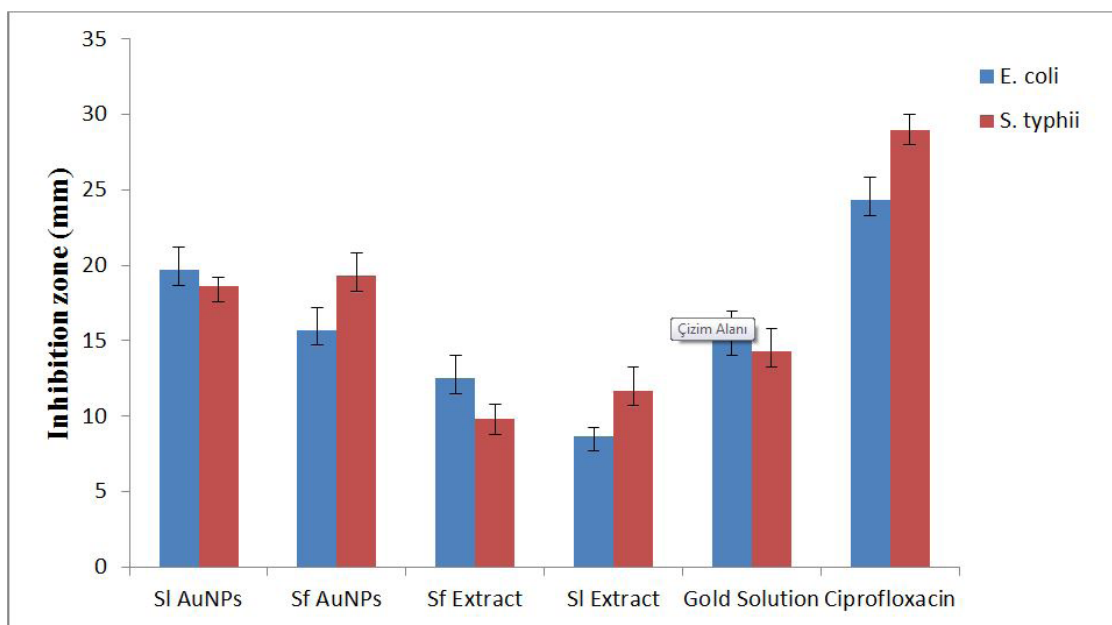


**Figure 8c.** A graphical representation of the mean zones of inhibition formed during the disc diffusion method of antimicrobial test. The data is represented as the mean  $\pm$  standard deviation of the at least n=3 replicates of the experiment.

very strong diffraction peak at 39.512 degrees is considered to be of [111] facet of the face centered cubic structure (Figure 6b), while the diffraction peaks of other gold peaks are found to be much weaker compared to gold nanoparticles synthesized using *S. filamentosa*. It is imperative to note that the ratio of intensity between [200] and [111] peaks, [220] and [111] peaks as well as [311] and [111] peaks are much smaller compared to the intensity ratios of gold nanoparticles synthesized using *S. filamentosa*. Presence of those peaks confirm the development of purified AuNPs without any impurity. Additionally, the pattern shows that the AuNPs was

obtained from natural sources. Results obtained from our study are in agreement with many similar studies and supports the previous findings of Philip [28] that revealed the crystalline nature of gold to be like that of circular rings.

#### Antioxidant Activity of Gold Nanoparticles

Antioxidant activity of the synthesized AuNPs for both extract were studied using DPPH free radical scavenging activity assay. In addition, the results obtained from the study were shown in Figure 7. Both nanoparticles showed significant activity but *S. filamentosa* AuNPs

**Table 2.** Comparison of the AuNPs synthesised using *S. filamentosa* and *S. lomentaria*

Algae species	Colour change	UV-Vis spectroscopy	Particle size distribution	Antibacterial activity	References
<i>Turbinaria conoides</i>	Ruby red	538 nm	2-19 nm	No inhibition formed against marine biofilm forming bacteria strains.	Vijayan et al., (2014) [36]
<i>Stoechospermum marginatum</i>	Ruby red	550 nm	<100 nm	Maximum inhibition against <i>E. faecalis</i>	Rajathi et al., (2012) [37]
<i>Galaxaura elongata</i>	Ruby red	536 nm (powder) 535 nm (extract)	2-100 nm	Maximum inhibition against <i>K. pneumoniae</i>	Abdel-Raouf et al., (2017) [38]
<i>Padina tetrastromatica</i>	Ruby red	550 nm	20-90 nm	High zone of inhibition against <i>S. aureus</i> and <i>P. aereginosa</i> .	Kayalvizhi et al., (2014) [39]
<i>Turbanaria ornate</i>	Ruby red	~550 nm	20-90 nm	Maximum zone of inhibition against <i>S. aureus</i>	Kayalvizhi et al., (2014) [39]
<i>Sargassum polycystum</i>	Ruby red	534 nm	50-80 nm	Maximum inhibition zone against <i>E. coli</i>	Dhas et al., (2014) [40]
<i>S. filamentosa</i>	pink	536 nm	<100 nm	Maximum inhibition zone against <i>S. typhi</i>	Present Study

revealed higher antioxidant activity ( $IC_{50} = 38.84 \mu\text{g}/\text{mL}$ ) compared to *S. lomentaria* ( $IC_{50} = 32.804 \mu\text{g}/\text{mL}$ ) and this might be as a result of biomolecules present in the extract. Antioxidant activity that is demonstrated by nanoparticles has to do with organic biomolecules present within the extract used during the nanoparticle synthesis as a chelating agent [29]. Additionally, studies reveal that high surface to volume ration are the reason for free radical scavenging activity of various synthesized nanoparticles [30, 31].

### Antimicrobial Activity

Antimicrobial potential of the synthesized AuNPs were investigated using agar well diffusion assay. Minimum inhibition concentration (MIC) and mean zone of inhibition (diameter in mm) were evaluated against *E. coli* and *S. typhi* and the result of the MIC was presented in Table 1 and mean zone of inhibition was represented in Figure 8a-d. The MIC for both was found nanoparticles was found to be SI AuNPs and Sf AuNPs gave the higher zone of inhibition when compared with the plant extract and

gold nanoparticles solution. Sf AuNPs revealed highest zone of inhibition against *S. typhi* when compared with SI AuNPs. Differences in the zone of inhibition between the two nanoparticles could be as a results of the difference in the biomolecules presents in the plants.

The antibacterial properties of the gold nanoparticles synthesised using *S. lomentaria* and *S. filamentosa* was tested against two strains of bacteria that are food borne (*E. coli* and *S. typhi*) and the visual observation showed that there were zones of inhibition formed around the nanoparticle solution and as shown in Figure 8.

Inhibitory action of nanoparticles differs and it has been reported to be based on surface area, size, biomolecule constituents coated on the AuNPs and the species [32]. Both SI AuNPs and Sf AuNPs revealed more inhibition on *S. typhi* than on *E. coli* and this could be as result of differences in the bacterial membrane structure, Gram positive bacteria, peptidoglycan layers are very thick than Gram negative bacteria [33]. Additionally, studi-

es reported that, AuNPs exert its anti-microbial effect through changing the membrane potential and inhibition of F-type ATP synthase, which could lead to decrease in ATP level and decline in the metabolism of microbes [34]. AuNPs can also inhibit ribosomal RNA protein S10 subunit through modification of 4, 6-diaminopyrimidine thiol, which can serve as bacterial tRNA base, and it has the proficiency to inhibit tRNA function which could lead to the loss of protein synthesis [35].

The inhibition zone of the 19.7 mm and 15.7 mm was recorded for *E. coli* against the *S. lomentaria* AuNPs and *S. filamentosa* AuNPs respectively (Figure 8c). Simultaneously 18.6 mm and 19.3 mm was recorded for *S. typhi* against the *S. lomentaria* AuNPs and *S. filamentosa* AuNPs respectively. A similar study done on the synthesis of gold nanoparticles using a *G. elongata* ethanoic extract showed that more of inhibition were formed against *E. coli*, *K. pneumoniae* and multiple antibiotic resistant *S. aureus* with the maximum zones measuring between 17 mm and 16 mm respectively [38]. A report done by Kayalvizhi et al., indicated that capped gold nanoparticles can interact with bacterial cell walls and interrupted the metabolism of the bacterial cell due to the presence of phytochemicals that are present in the in the plant extract. The small size of the nanoparticles allowed them to enter the cell membrane and interact with the mitochondria and other organelles since the nanoparticles do not degrade the cell wall [39]. The *S. lomentaria* gold nanoparticles showed the greatest antibacterial effect against *E. coli*. The gold nanoparticles synthesized using the *S. filamentosa* also showed a great antibacterial effect against *S. typhi*. The p values are  $p < 0.05$ . Thus, there is a significant difference in the zone of inhibition zone formed by the gold nanoparticles synthesized using *S. lomentaria* and there is no significant difference between the gold solution and the gold nanoparticles synthesized using the *S. filamentosa* as the p value is greater than the critical values.

### Comparison of the Gold Nanoparticles

The gold nanoparticles formed using *S. lomentaria* form a ruby red colour whereas the *S. filamentosa* synthesized nanoparticles form a pink colour. This is due to the different surface plasmon resonance which also UV-Vis peaks at 536 and 540 nm. On average the nanoparticles are relatively equal as shown in Table 2. There is no significant difference in the bands shown by the FT-IR spectra showing that there are approximately similar bi-

omolecules. Our study revealed that, the two species of seaweed have antibacterial activity against *S. typhimurium* and *E. coli*. After the synthesis of the nanoparticles, the test showed that there is a significant difference in the inhibition zones formed by extracts and those formed by the nanoparticles. According to literature there is not much variation in the functional groups found in the bioactive compounds of most seaweed compounds, therefore Table 2 shows some of the variations in antibacterial activity, UV-Vis spectroscopy, colour change and particle size of AuNPs synthesised using various seaweed species.

Furthermore, antioxidant study using DPPH free radical scavenging activity revealed *S. filamentosa* to have higher antioxidant activity ( $IC_{50} = 38.84 \mu\text{g/mL}$ ) when compared to *S. lomentaria* ( $IC_{50} = 32.804 \mu\text{g/mL}$ ) and this might be as a result of biomolecules present in the extract.

### Conclusion

Overall, AuNPs were synthesized using aqueous extract of *S. filamentosa* and *S. lomentaria* through a constant, and eco-friendly green route. Gold reduction using the two species of seaweeds is effective as the biomolecules required for the reduction of the gold ions are available in the extract solution. The successful synthesis of AuNPs using aqueous extract of *S. filamentosa* and *S. lomentaria* was confirmed using UV-vis, Zeta sizer, FTIR and XRD. The UV-Vis result revealed absorption peak at range of 540 nm. The biosynthesized nanoparticle showed strong antioxidant activity with  $IC_{50}$  value of 38.84 and 32.804  $\mu\text{g/mL}$  for *S. filamentosa* and *S. lomentaria* respectively. Additionally, synthesized AuNPs showed significant antimicrobial activity against *E. coli* and *S. typhi*.

---

### References

---

1. S. Hua, M.B.C. de Matos, J.M. Metselaar, G. Storm, Current Trends and challenges in the clinical translation of nanoparticulate nanomedicines: pathways for translational development and commercialization, *Front Pharmacol.*, 9 (2018) 790.
2. P.K. Jain, X. Huang, I.H. El-Sayed, M.A. El-Sayed, Noble metals on the nanoscale: optical and photothermal properties and applications in imaging, sensing, biology, and medicine, *Acc. Chem. Res.*, 41 (2008) 1578-1586.
3. P. Mohanpuria, N.K. Rana, S.K. Yadav, Biosynthesis of nanoparticles: technological concepts and future applications, *J. Nanopart. Res.*, 10 (2008) 507-517.

4. P. Khandel, R.K. Yadaw, D.K. Soni, L.Kanwar, S.K. Shahi, Biogenesis of metal nanoparticles and their pharmacological applications: present status and application prospects, *J. Nanostructure Chem.*, 8 (2018) 217-254.
5. V.G. Kumar, S.D. Gokavarapu, A. Rajeswari, T.S. Dhas, V. Karthick, Z. Kapadia, T. Shrestha, I.A. Barathy, A. Roy, S. Sinha, Facile green synthesis of gold nanoparticles using leaf extract of antidiabetic potent *Cassia auriculata*, *Colloids Surf. B.*, 87 (2011) 159-163.
6. D. Kavaz, S. Lamido, H. Umar, Antimicrobial activity of silver nanoparticles synthesized via green chemistry, *the Russian Academic Journal*, 34 (2015) 36-44.
7. H.Y. El-Kassas, M.M. El-Sheekh, Induction of the synthesis of bioactive compounds of the marine alga *Tetraselmis tetrahele* (West) Butcher grown under salinity stress, *Egypt J. Aquat. Res.*, 42 (2016) 385-391.
8. S. Naraginti, Y. Li, Preliminary investigation of catalytic, antioxidant, anticancer and bactericidal activity of green synthesized silver and gold nanoparticles using *Actinidia deliciosa*, *J. Photochem. Photobiol. B Biol.*, 170 (2017) 225-234.
9. Z. Salari, F. Danafar, S. Dabaghi, S.A. Ataei, Sustainable synthesis of silver nanoparticles using macroalgae *Spirogyra varians* and analysis of their antibacterial activity, *J. Saudi Chem. Soc.*, 20 (2016) 459-464.
10. K.Vijayaraghavan, T. Ashokkumar, Plant-mediated biosynthesis of metallic nanoparticles: A review of literature, factors affecting synthesis, characterization techniques and applications, *J. Environ. Chem. Eng.*, 5 (2017) 4866-4883.
11. A.M. Alkilany, C.J. Murph, Toxicity and cellular uptake of gold nanoparticles: what we have learned so far? *J. Nanopart. Res.*, 12 (2010) 2313-2333.
12. M. Rajan, K. Meena, D. Philip, Shape tailored green synthesis and catalytic properties of gold nanocrystals, *Spectrochim. Acta. Part A: Mol. Biomol. Spectrosc.*, 118 (2014) 793-799.
13. Y. Li, H.J. Schluessener, S. Xu, Gold nanoparticle-based biosensors. *Gold Bull.*, 43 (2010) 29-41.
14. K. Saha, S.S. Agasti, C. Kim, X. Li, V.M. Rotello, Gold nanoparticles in chemical and biological sensing, *Chem Rev.*, 112 (2012) 2739-2779.
15. L. Dykman, N. Khlebtsov, Gold nanoparticles in biomedical applications: recent advances and perspectives, *Chem. Soc. Rev.*, 41 (2012) 2256-2282.
16. P. Sandström, M. Boncheva, B. Åkerman, Nonspecific and thiol-specific binding of DNA to gold nanoparticles. *Langmuir*, 19 (2013) 7537-7543.
17. M. Znati, H.B. Jannet, S. Cazaux, J. Bouajila, Chemical Composition, Biological and Cytotoxic Activities of Plant Extracts and Compounds Isolated from *Ferula lutea*, *Molecules*, 19 (2014) 2733-2747.
18. K. Vijayaraghavan, A. Mahadevan, M. Sathishkumar, S. Pavagadhi, R. Balasubramanian, Biosynthesis of Au (0) from Au(III) via biosorption and bioreduction using brown marine alga *Turbinaria conoides*, *Chem. Eng. J.*, 167 (2011) 223-227.
19. M. Ramakrishna, B.D. Rajesh, G. Robert, S. Chandra, G. Rao, Green synthesis of gold nanoparticles using marine algae and evaluation of their catalytic activity, *J. Nanostructure Chem.*, 6 (2016) 1-13.
20. D. Mubarak Ali, N. Thajuddin, K. Jeganathan,, M. Gunasekaran,, Plant extract mediated synthesis of silver and gold nanoparticles and its antibacterial activity against clinically isolated pathogens, *Colloid Surface B.*, 85 (2011) 360-365.
21. D. Inbakandan, R. Venkatesan, S.A. Khan, Biosynthesis of gold nanoparticles utilizing marine sponge *Acanthella elongate*, *Colloids Surf. B.*, 81 (2010) 634-639.
22. S.A. Aromal, D. Philip, Benincasa hispida seed mediated green synthesis of gold nanoparticles and its optical nonlinearity, *Physica E. Low. Dimens. Syst. Nanostruct.*, 44 (2012) 1329-34.
23. K.F. Princy, A. Gopinath, Optimization of physicochemical parameters in the bio fabrication of gold nanoparticles using marine macro algae *Padina tetrastromatica* and its catalytic efficacy in the degradation of organic dyes, *J. Nanostruct. Chem.*, 8 (2018) 333-342.
24. R. Geetha, T. Ashokkumar, S. Tamilselvan, K. Govindaraju, M. Sadiq, G. Singaravelu, Green synthesis of gold nanoparticles and their anticancer activity, *Cancer Nanotechnol.*, 4 (2013) 91-98.
25. N. Kuyucak, B. Volesky, Accumulation of gold by algal biosorbent, *Biorecovery*, 1 (1989) 189-204.
26. P. Karupaiya, E. Satheeshkumar, W.T. Chao, L.Y. Kao, E.C. Chen, H.S. Tsay, Antimetastatic activity of biologically synthesized gold nanoparticles on human fibrosarcoma cell line HT-1080, *Colloid Surface B.*, 110 (2013) 163-70.
27. C.H. Ramamurthy, M. Padma, I.D. Samadanam, R. Mareeswaran, A. Suyavaran, M.S. Kumar, K. Premkumar, C. Thirunavukkarasu, The extra cellular synthesis of gold and silver nanoparticles and their free radical scavenging and antibacterial properties, *Colloid Surface B.*, 102 (2013) 808-815.
28. D. Philip, Honey mediated green synthesis of gold nanoparticles, *Spectrochim. Acta A*, 73 (2009) 650-653.
29. H. Umar, D. Kavaz, N. Rizaner, Biosynthesis of zinc oxide nanoparticles using *Albizia lebbek* stem bark, and evaluation of its antimicrobial, antioxidant, and cytotoxic activities on human breast cancer cell lines, *Int. J. Nanomed.*, 14 (2019) 87-100.
30. G. Balasubramani, R. Ramkumar, N. Krishnaveni, A. Pazhanimuthu, T. Natarajan, R.Sowmiya, P. Perumal, Structural characterization, antioxidant and anticancer properties of gold nanoparticles synthesized from leaf extract (decoction) of *Antigonon leptopus*, *J. Trace Elem. Med. Biol.*, 30 (2015) 83-89.
31. M.K. Swamy, M.S. Akhtar, S.K. Mohanty, U.R. Sinniah, Synthesis and characterization of silver nanoparticles using fruit extract of *Momordica cymbalaria* and assessment of their in vitro antimicrobial, antioxidant and cytotoxicity activities, *Spectrochim. Acta A*, 151 (2015) 939-944.
32. T.J.I. Edison, M.G. Sethuraman, Instant green synthesis of silver nanoparticles using *Terminalia chebula* fruit extract and evaluation of their catalytic activity on reduction of methylene blue, *Process Biochem.*, 47 (2012) 1351-1357.
33. M.M. Mohamed, S. A. Fouad, H.A. Elshoky, G.M. Mohammed, T.A. Salaheldin, Antibacterial effect of gold nanoparticles against *Corynebacterium pseudotuberculosis*, *Int. J. Vet. Sci. Med.*, 5 (2017) 23-29.
34. S. Prabukumar, C. Rajkuberan, G. Sathishkumar, M. Illaiyaraja, S. Sivaramkrishnan, Biogenic gold nanoparticles synthesized using *Crescentia sujete* L. and evaluation of their different biological activities, *Biocatal. Agric. Biotechnol.*, 11 (2017) 75-82.
35. M. Umadevi, T. Rani, T. Balkrishnan, R. Ramanibai, Antimicrobial activity of silver nanoparticles under an ultrasonic field, *Int. J. Pharm. Sci. Nanotechnol.* 4 (2011) 1491-1496.

36. S.R. Vijayan, P. Santhiyagu, M.S. Singamuthu, N. Kumari, R. Anila, R. Jayaraman, K. Ethiraj, Synthesis and characterization of silver and gold nanoparticles using aqueous seaweed; *Turbinaria conoides* and their antimicrobial activity, *The Scientific World Journal*. 2014 (2014) Article ID 938272. <http://dx.doi.org/10.1155/2014/938272>.
37. F.A.A. Rajathi, C. Parthiban, G.V. Kumar, P. Anantharaman, Biosynthesis of antibacterial gold nanoparticles using brown alga *Stoechospermum marginatum*, *Spectrochim. Acta A.*, 99 (2012) 166-173.
38. N. Abdel-Raouf, N.M. Al-Enazi, I.B.M. Ibraheem, Green biosynthesis of gold nanoparticles using *Galaxaura elongata* and characterization of their antibacterial activity, *Arab. J. Chem.*, 10 (2017) 3029-3039.
39. K. Kayalvizhi, N. Asmathunisha, V. Subramanian, K. Kathiresan, Purification of silver and gold nanoparticles from two species of brown seaweeds (*Padina tetrastromatica* and *Turbinaria ornata*), *J. Med. Plants Stud.*, 2 (2014) 32-37.
40. T.S. Dhas, V.G.Kumar, T. Malyalagan, K. Govindaraju, Biofabrication of Gold Nanoparticles Using *Sargassum polycystum* and their Antibacterial Activity, *Adv. Chem. Lett.*, 2 (2015) 31-35.